Supramolecular Structure, Physical Properties, and Langmuir–Blodgett Film Formation of an Optically Active Liquid-Crystalline Phthalocyanine

Cornelus F. van Nostrum, Anton W. Bosman, Gerwin H. Gelinck, Pieter G. Schouten, John M. Warman, Arno P. M. Kentgens, Marinus A. C. Devillers, Andries Meijerink, Stephen J. Picken, Ulrich Sohling, Arend-Jan Schouten, and Roeland J. M. Nolte*

Abstract: The structure and physical properties of optically active, metal-free 2,3,9,10,16,17,23,24-octa(*S*-3,7-dimethyloctoxy)phthalocyanine ((*S*)-Pc(8,2)) are reported and compared with those of the phthalocyanine with (*R,S*) side chains (mixture of 43 stereoisomers). Unlike the latter compound, (*S*)-Pc(8,2) lacks a crystalline phase. A freshly prepared sample is in a distorted mesophase and reorganizes irreversibly to a more ordered phase above 65 °C. X-ray diffraction and circular dichroism studies indicate that the molecules are stacked in columns which have a hexagonal arrangement and a left-handed helical superstructure, that is, a novel chiral D_h^* mesophase. Solid state NMR measurements reveal that the phthalocyanine units in the columns begin to vibrate laterally when the temperature is increased. At 111 °C ($D_h^* \rightarrow D_r$ transition) they start to rotate around their columnar axes and at the same time the side chains become liquidlike. Energy migration is very efficient in the chiral D_h^* phase and also in the frozen mesophase below 3 °C, as follows from luminescence spectroscopy. Intracolumnar charge transport, studied by the time-resolved microwave conductivity technique, turns out to be slower in the helically distorted columns than in linear columns. (*S*)-Pc(8,2) forms a very stable bilayer at the air–water interface, which can be transferred to give a high quality Langmuir–Blodgett film. The fact that this phthalocyanine is mesogenic at room temperature is thought to be responsible for this behavior.

Keywords
chiral mesophases · Langmuir–Blodgett films · liquid crystals · phthalocyanines · supramolecular chemistry

Introduction

Since the discovery by Chandrasekhar et al. in 1977 that disclike molecules can form a columnar liquid-crystalline phase,[1] a large number of compounds have been reported to display this mesophase structure. Among the most studied examples are truxenes, triphenylenes, and phthalocyanines (Pcs).[2] In general, molecules forming a columnar mesophase are built up from a disc-shaped rigid core which is substituted with long flexible hydrocarbon chains. Pcs are particularly interesting building blocks because they can have special catalytic, optical, and gas-sensing properties.[3] Moreover, when organized in stacks they may show one-dimensional energy migration and charge transport.[3] The first mesomorphic Pc was synthesized by Piechocki et al. in 1982.[4] Since then, we and others have investigated the mesophase structure of a wide variety of Pcs and porphyrins,[5] including molecules that are substituted with eight linear alkyl,[5c] alkoxymethyl,[4, 5d, e] and alkoxy[5e–g] chains. All these compounds display a transition from the solid phase to the mesophase at elevated temperatures. Powder X-ray diffraction measurements have revealed that the macrocycles are stacked in columns in the solid phase. The Pc molecules are tilted with respect to the columnar axis and have a center-to-center distance along this axis of 4.3 Å.[6] In the mesophase the molecules are also arranged in columnar stacks, but the Pc planes are now perpendicular to the columnar axis with a center-to-center distance of about 3.4 Å. The columns are hexagonally ordered and the mesophase is classified as being a D_h phase.[5f, 7, 8] With the help of temperature-dependent solid-state ^{13}C NMR measurements we were able to show that the molecules rotate around their columnar axes in the mesophase of octaundecoxy Pc.[9] The alkoxy side chains were found to have a liquidlike order.

One-dimensional energy (exciton)[10] and charge migration[5f, 11] in mesomorphic Pcs have been extensively studied. Information about intra- and intercolumnar charge transport

[*] Prof. Dr. R. J. M. Nolte, C. F. van Nostrum, A. W. Bosman, G. H. Gelinck
Department of Organic Chemistry, NSR Center
University of Nijmegen, 6525 ED Nijmegen (The Netherlands).
Telefax: Int. code + (80) 553-450
P. G. Schouten, Dr. J. M. Warman
IRI, Delft University of Technology (The Netherlands)
Dr. A. P. M. Kentgens
SON/NWO HF NMR Facility, University of Nijmegen (The Netherlands)
Dr. M. A. C. Devillers.
Experimental Solid State Physics, University of Nijmegen (The Netherlands)
Dr. A. Meijerink
Physics Laboratory, University of Utrecht (The Netherlands)
Dr. S. J. Picken
Akzo Nobel Central Research, Physical Chemistry Department, Arnhem (The Netherlands)
Dr. U. Sohling, Dr. A. J. Schouten
Laboratory of Polymer Science, University of Groningen (The Netherlands)

  0570-0833/95/0303-0171 $ 30.00+.25/0

was obtained by the time-resolved microwave conductivity (TRMC) technique.[11f-i] Ionization with short (nanosecond) pulses of high-energy electrons was used to create charge carriers in the bulk material. In the case of octaalkoxy Pcs the end-of-pulse conductivity decreased sharply at the solid-to-mesophase transition.[11f,i] This effect was explained by an increase of the molecular motion in the mesophase, which more than counteracted the expected increase in charge migration due to the better $\pi-\pi$ overlap between the Pc rings. At the mesophase to isotropic phase transition the conductivity dropped to zero; this supports the idea that a columnar structure is necessary for charge transport.[11g] From the observation that the lifetime of the conductivity transients in the TRMC experiments is exponentially dependent on the length of the alkoxy chains, it was concluded that intercolumnar transport takes place in a tunneling process through the hydrocarbon mantles.[11f-i]

Most of the Pcs studied so far become liquid crystalline at elevated temperatures only. The few examples that are liquid crystalline at room temperature have branched hydrocarbon substituents.[5b,e,g,i,12] Branching probably introduces disorder and hence a decrease in the transition temperature.[13] We recently synthesized the branched phthalocyanine (*R,S*)-Pc(8,2) and studied the liquid crystalline properties of this compound (Table 1).[11i,12] At room temperature, (*R,S*)-Pc(8,2) has a supercooled mesophase that crystallizes in a couple of hours. This compound was prepared from a racemic starting material, and the product is therefore a mixture of a large number of stereoisomers, namely, 43 (16 pairs of enantiomers and 11 meso compounds). As such a mixture is unfavorable for studying the relation between the molecular structure of the compound and its material properties, we synthesized the optically active phthalocyanine, with the eight chiral centers in the side chains all in the (*S*) configuration ((*S*)-Pc(8,2)).[14] Only a few examples of optically active discotic mesogens are known. Destrade et al. have described the synthesis of chiral esters of triphenylenes and truxenes exhibiting a columnar mesophase.[15] An aligned sample of one of the former compounds was studied by X-ray diffraction, which clearly indicated that the columns were helically distorted.[16] Ringsdorf et al. have suggested that films of polymers of chiral triphenylenes contain helical superstructures.[17] An optically active mesogenic dibenzopyrene that displays ferroelectrical switching has been reported.[18] One example of an optically active mesogenic Pc has been published in the literature.[5e] No evidence of a chiral superstructure was reported in this case. Noteworthy also are the recently reported optically active binaphthol substituted Pcs, which are not liquid crystalline, but show interesting circular dichroism activity in solution.[19]

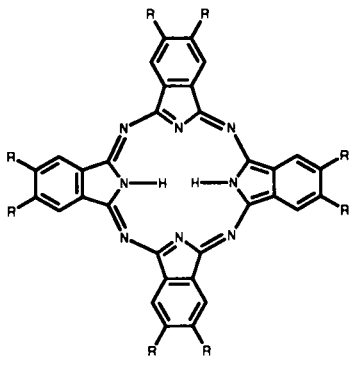

In this paper we report on the structure and physical properties of optically active (*S*)-Pc(8,2). X-ray and solid state NMR studies are presented as well as studies of intramolecular energy and charge transport. The results are compared with those obtained with (*R,S*)-Pc(8,2). In addition to this, we will show that Langmuir–Blodgett (LB) films of excellent quality can be prepared from (*S*)-Pc(8,2).

Table 1. Phase-transition temperatures and enthalpy changes determined by DSC, and structural assignments from X-ray diffraction and polarization microscopy [a].

Compound	Transition	T/°C [b]	ΔH/kJ mol^{-1}
(*R,S*)-Pc(8,2)	K → D_h [c]	70	54.6
	$D_h \leftrightarrow I$	295(293)	8.3
(*S*)-Pc(8,2)	A → D_h^* [d]	45–65	8.2
	$D \leftrightarrow D_h^*$	14(3)	6.4
	$D_h^* \leftrightarrow D_r$	111(95–75)	3.1
	$D_r \leftrightarrow I$	295(295)	10.9

[a] A: amorphous phase, K: crystalline phase, D_h: hexagonal columnar mesophase, D_h^*: chiral D_h phase, D: unknown columnar mesophase, D_r: rectangular columnar mesophase, I: isotropic phase. [b] Temperatures as observed in heating and cooling (in parentheses) DSC runs. [c] The reverse transition to the crystalline phase was not observed by DSC, but other experiments (see text) show that crystallization takes place at room temperature within a couple of hours. [d] Irreversible phase transition, only observed on heating a freshly precipitated sample.

Experimental Procedure

Synthesis: Metal-free 2,3,9,10,16,17,23,24-octa(*R,S*-3,7-dimethyloctoxy)phthalocyanine ((*R,S*)-Pc(8,2)) was prepared as described previously [12]. The optically active derivative, (*S*)-Pc(8,2), was synthesized by an analogous procedure, starting from optically pure (*S*)-citronellol, which was purchased from Aldrich and used without further purification. The spectroscopic data of (*S*)-Pc(8,2) were similar to that of (*R,S*)-Pc(8,2) [12]. Thermogravimetric analyses (TGA) showed that decomposition of (*S*)-Pc(8,2) starts at 280 °C in air and at 350 °C under an inert atmosphere. $[\alpha]_{546}^{20} = -1200$ ($c = 0.001$ in $CHCl_3$); anal. $C_{112}H_{178}N_8O_8$ (1764.7): calcd C 76.23, H 10.17, N 6.35; found C 76.15, H 10.11, N 6.31%.

Measurements: Differential scanning calorimetry (DSC) data were obtained with a Mettler DSC 12E and a Perkin-Elmer 7 Series Thermal Analysis System. The measurements were carried out under an inert atmosphere with 3–7 mg samples and heating and cooling rates of 1–20 °C min^{-1}. TGA was carried out on a Perkin Elmer 7 Series Thermal Analysis System and a Perkin Elmer System 4 under ambient and inert atmospheres. For polarization microscopy (PM) a Leitz Orthoplan polarization microscope was used, equipped with a Mettler FP80/FP82 Hot Stage. Small-angle X-ray scattering (SAXS) measurements were recorded with a Kiessig Camera (focal distance 8.01 cm, $Cu_{K\alpha}$ source with a wavelength of 1.5418 Å).
High-resolution solid-state NMR spectra were obtained on a Bruker AM 500 spectrometer (proton frequency 500.14 MHz, carbon frequency 125.7 MHz) equipped with a Doty 5 mm MAS probe. Magic angle spinning speeds of approximately 4200 Hz were employed. Temperatures were measured with a Bruker VT 100 instrument. Spectra were recorded using single-pulse excitation and high-power proton decoupling. The spectra below −10 °C were obtained with cross-polarization (CP) with 3 ms contact time, a relaxation delay of 4 s, and a proton pulse of 5.1 µs. 500–4000 FID's were accumulated per spectrum. Adamantane was used as secondary reference with respect to TMS for the calibration of the spectra.
Luminescence measurements were carried out on a Spex Fluorolog 2 spectrofluorometer equipped with a Xe lamp, a red-sensitive photomultiplier (Hamamatsu R928), a liquid helium flow cryostat (Oxford CF1204), and a home-made high-temperature cell. Emission spectra were recorded after excitation in the Q band at 560 nm at temperatures of 4–400 K.
The pulse-radiolysis time-resolved microwave conductivity (PR-TRMC) measurements were carried out as described elsewhere [11i].

Langmuir–Blodgett Film Formation and Characterization: Monolayers at the air–water interface were studied by measuring pressure–area isotherms on a computer-controlled Lauda Film Balance (FW2) with water, purified by a Milli-Q filtration system, as the subphase. The samples were dissolved in chloroform (spectroscopic quality, ca. 1 mg mL^{-1}), spread on the water surface, and isotherms were recorded at a compression speed of ca. 10 Å^2 molecule^{-1} min^{-1}.
Quartz, glass, and silicon substrates were cleaned ultrasonically with chloroform, treated with concentrated sulfochromic acid at 80 °C for 2 h, washed several times with Milli-Q water, cleaned again ultrasonically in acetone and in chloroform, and finally stored in methanol. Before use the substrate was rinsed with chloroform, partially hydrophobized by treatment with a boiling mixture of chloroform and hexamethyldisilazane, and finally rinsed with chloroform. Gold substrates were obtained by sputtering a gold layer 500 Å thick onto the cleaned glass slides. Zinc sulfide plates, also used as substrates, were cleaned by washing thoroughly with chloroform. Deposition was performed by vertically dipping the substrate through

0570-0833/95/0303-0172 $ 30.00+.25/0 Chem. Eur. J. 1995, 1, No. 3

a stabilized monolayer at a constant surface pressure and temperature with a speed of 5–10 mm min^{-1}.

UV/Vis measurements were carried out with a SLM-Aminco 3000 diode array spectrophotometer. Transmission (TM) and grazing incidence reflection (GIR) Fourier-transform infrared (FT-IR) spectra were recorded on a Bruker IFS-88 FT-IR spectrometer at 4 cm^{-1} resolution by the method of Arndt [20]; cycles of 1000 scans were used. The TM spectra were taken from a 10-layer film on both sides of zinc sulfide substrates, and the GIR spectra were taken from a 20-layer film on gold substrates. The films were studied by means of polarization microscopy with the microscope described above. Film thicknesses and refractive indices were measured on a Gaertner L117-C single-wavelength ellipsometer (λ = 632.8 nm). Small angle X-ray diffraction was performed with a Siemens D-500 powder diffractometer, equipped with a graphite monochromator at the detector side, and $Cu_{K\alpha}$ radiation with a wavelength of 1.542 Å.

Circular dichroism (CD) spectra were recorded on a JASCO J-600 spectropolarimeter at temperatures between −10 and 100 °C. The molecular ellipticity, $[\theta]$, is defined by Equation (1) [21]:

$$[\theta] = \frac{[\Psi]M}{100} \quad (1)$$

where M = molecular mass and Ψ = measured ellipticity (degrees), which is defined by Equation (2):

$$[\Psi] = \frac{\Psi}{Ld} \quad (2)$$

where L = film thickness (dm) and d = density (g mL^{-1}). The product of L and d in Equation (2) can be calculated according to Equation (3):

$$Ld = \frac{Mn}{6 \times 10^8 A} \quad (3)$$

where n = number of monolayers in the film and A = area per molecule (Å^2) from the pressure–area isotherm. The combination of Equations (1)–(3) gives Equation (4):

$$[\theta] = \Psi \frac{6 \times 10^6 A}{n} \quad (4)$$

Equation (4) can be generally applied for the calculation of the molecular ellipticity of LB films.

Results

Phase Behavior: DSC measurements were performed to study the phase behavior of (*S*)-Pc(8,2). The phase transition temperatures and enthalpy changes are given in Table 1. On heating a freshly precipitated sample of (*S*)-Pc(8,2), a broad endothermic peak was observed between 45 and 65 °C. This peak did not appear in the second and further heating scans. (*R,S*)-Pc(8,2) is known to behave similarly, namely, an irreversible transition at 70 °C was observed, which was attributed to a transition from crystalline (K) to mesophase (M).[12] However, in the case of (*S*)-Pc(8,2) the peak is less sharp and the transition enthalpy much lower, which makes a K → M transition less likely. On further heating a second small transition was found at 111 °C. The reverse transition occurs slowly; only occasionally was a weak and broad DSC peak observed between 95 and 75 °C. At 295 °C the transition to the isotropic phase took place. On cooling (*S*)-Pc(8,2) below room temperature a reversible phase transition was found at 3 °C, which was accompanied by a small enthalpy effect. The second and further DSC runs were similar to the first one, except that the transition at between 45 and 65 °C was absent.

When (*S*)-Pc(8,2) was slowly cooled down from the isotropic phase, a mosaic texture appeared under the polarization microscope, which is characteristic for a columnar mesophase (Fig. 1, left). When the material was further cooled down slowly to 70 °C, small cracks appeared in the texture; this indicates that a transition to a more ordered mesophase took place. However, when the material was quickly cooled down form the isotropic phase to room temperature a very characteristic texture was observed with spiral concentric rings (Fig. 1, right). This result is a first indication of the presence of a chiral mesophase. Spiral textures have also been reported for chiral triphenylenes.[22]

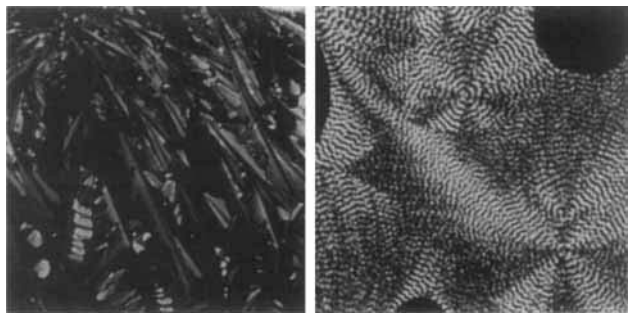

Fig. 1. Textures of (*S*)-Pc(8,2) observed between crossed polarizers at 250 °C after slowly cooling from the isotropic phase (left) and at room temperature after quickly cooling (right).

The structures of two of the stable phases of (*S*)-Pc(8,2) were determined by powder X-ray diffraction measurements at 80 and 180 °C. Due to restrictions of the apparatus, the structure of the phase below room temperature could not be determined. The results are shown in Table 2. A number of reflections of (*S*)-Pc(8,2) at 80 °C are similar to those of (*R,S*)-Pc(8,2); this indicates that both compounds have a D_h phase. The additional weak reflections on both sides of the 3.4 Å reflection observed in the case of (*S*)-Pc(8,2) indicate the presence of an extra periodicity along the columnar axis. The columnar structure can be described in terms of the superspace approach of de Wolff, Janner, and Janssen,[23] in which the periodicity is described mathematically in a higher dimensional Euclidean space. In the case of a single modulation, the set (*hklm*) expresses the components of a reciprocal wave vector $\boldsymbol{K}$ in terms of four fundamental periodicities. In three dimensions $\boldsymbol{K} = h\boldsymbol{a}^* + k\boldsymbol{b}^* + l\boldsymbol{c}^* + m\boldsymbol{q}$, where $\boldsymbol{a}^*$, $\boldsymbol{b}^*$, and $\boldsymbol{c}^*$ refer to the basic structure and $\boldsymbol{q}$ is the wave vector of the modulation. For $m = 0$ the unmodulated structure is obtained, that is, a hexagonal pattern of columns and an average intracolumnar stacking distance of 3.4 Å. The satellite reflections around 3.4 Å, S_1 and S_2, are the result of the recipro-

Table 2. Spacings from X-ray diffraction data (Å) and assigned Miller indices (*hklm*) of (*R,S*)-Pc(8,2) and (*S*)-Pc(8,2) at various temperatures [a].

(*hklm*)	(*R,S*)-Pc(8,2)	(*S*)-Pc(8,2)	
	20 °C	80 °C	180 °C
0002	–	27.44	–
1000	24.64	24.01	26.06
0100	24.64	24.01	23.13
0003	–	18.76	–
1100	15.59	15.32	–
2000	13.87	–	13.41
2100	10.44	10.16	–
3000	9.47	9.59	–
0011	–	3.63	–
0010	3.39	3.43	3.55
001−1	–	3.22	–
D	31.98	31.63	–
P	–	56.5	–

[a] *P* = helical periodicity. The largest *d* spacings are the most inaccurate ones, owing to large experimental errors. They were not included in the calculation of the values of the intercolumnar distance *D*.

cal summation of two independent periodicities, expressed in terms of a formula as $1/S_{1,2} = 1/3.4 + q/m$. If they are regarded as first order satellites ($m = \pm 1$), the extra periodicity along the columnar axis can be calculated to be 57 ± 4 Å. Each periodicity includes approximately 16 molecules. The extra reflections at low angles, 27.4 and 18.8 Å, can be indexed as (0002) and (0003), respectively. The columnar modulation is probably the result of a helical superstructure (see below). We denote this chiral phase as a D_h^* phase.

The X-ray diffraction measurements at 180 °C gave only a few reflections. The ones that were assigned to the columnar modulation at 80 °C had disappeared. The few low angle reflections could not be indexed according to a hexagonal lattice. They were consistent with a rectangular lattice; this suggests that a D_r phase is present above 111 °C. A similar phase transition has been reported for triphenylene hexa(dodecanoate) by Safinya et al.[24]

Solid-State NMR: Solid-state NMR experiments were carried out to gain insight into the structural and dynamic changes that occur at the phase transitions of (*S*)-Pc(8,2). For comparison, experiments were also performed with octa(dodecoxy)-phthalocyanine (Pc(12)).

Aromatic core signals: ^{13}C MAS NMR spectra of the aromatic core signals of (*S*)-Pc(8,2) showed a temperature dependence that could be correlated with the transitions found by DSC. Below -10 °C strong cross-polarization signals were recorded for all the core carbon atoms (Fig. 2a). The spectra were, however, significantly broader than the corresponding spectra of Pc(12) and the previously studied Pc(11).[9] This indicates that the structure of (*S*)-Pc(8,2) differs from the crystalline structure of Pc(11) and Pc(12) and is probably less ordered. We previously reported that the chemical shifts of the core carbons of Pc(11) are influenced by intermolecular ring current effects leading to well-resolved crystallographic splittings in the ^{13}C MAS NMR spectra of the crystalline state. In the present case such well-resolved splittings were absent, which indicates that there is a large distribution of different crystallographic sites. It is of interest that, for carbon atom C4 in (*S*)-Pc(8,2), the observed chemical shift difference between the solution spectrum and the spectrum in the solid state (Table 3) was much larger than for the corresponding carbon atoms in Pc(11)[9] and Pc(12) (results not shown). This suggests that in (*S*)-Pc(8,2) the shielding due to neighboring molecules is larger than in Pc(12) and Pc(11), which in turn points to a more slipped and/or eclipsed molecular stacking in (*S*)-Pc(8,2).

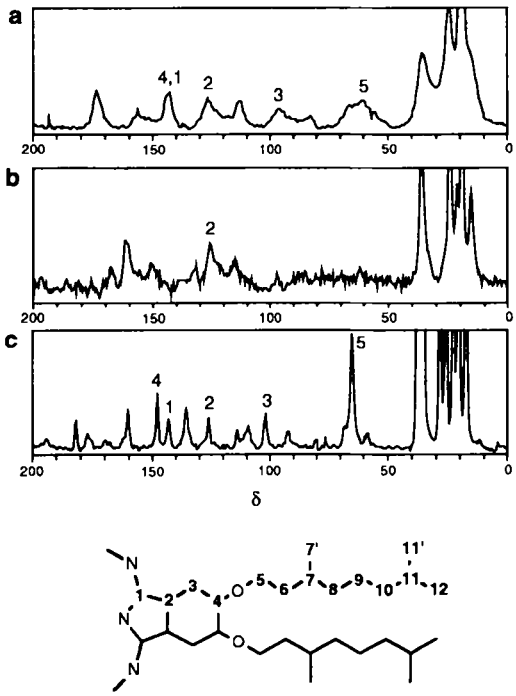

Fig. 2. Solid-state ^{13}C NMR spectra of (*S*)-Pc(8,2) a) at -60 °C with cross-polarization, b) at 25 °C with cross-polarization, and c) at 140 °C with direct pulse excitation. The labels used for spectral assignment are shown below the spectra. Peaks that are not numbered are spinning side bands.

Table 3. Observed ^{13}C chemical shifts for (*S*)-Pc(8,2) in $CDCl_3$ solution and in the solid state at various temperatures [a].

	C1	C2	C3	C4	C5	C6	C7	C7'	C8
$CDCl_3$	149	130.2	105.3	152.0	68.0	36.5	30.2	19.9	37.6
155 °C	144.3	127.3	103.0	148.8	–	–	–	–	–
115 °C	143.2	126.4	102.1	148.3	65.7	35.8	29.0	18.1	37.1
25 °C	–	–	–	–	63	–	28	17	–
−15 °C	–	126	–	146	–	–	–	–	–
−35 °C	–	126	–	144	63	–	–	17	–
−60 °C	–	127	–	144	–	–	–	–	–

[a] For the labeling of the carbon atoms see Figure 2.

At temperatures above -10 °C, close to the transition to the D_h^* phase, a gradual broadening of the carbon signals of the Pc core was observed. In fact, above room temperature no well-resolved spectrum could be obtained either with cross-polarization or single-pulse excitation (Fig. 2b). This line broadening may indicate that the structural disorder in the sample has increased or that the molecular motions become larger on the NMR time scale. The latter explanation seems to be more likely, given the fact that the lines gradually disappeared. If, for instance, the molecules start to move laterally, every carbon will experience a different chemical shift as a function of time due to the ring current effects of neighboring molecules. Depending on the time scale and the amplitude of these motions, this phenomenon can smear out the resonances of the carbon atoms of the core to such an extent that they become unobservable.

When the temperature was raised above 85 °C, close to the temperature of the $D_h^* \rightarrow D_r$ transition, the signals of the carbon core reappeared and well-resolved lines were observed for every carbon (Fig. 2c). At these temperatures cross-polarization was no longer effective, and the single-pulse excitation technique had to be applied. Similar observations were made at the crystalline-to-mesophase transition of Pc(11)[9] and Pc(12) (results not shown). We attribute the sudden decrease of the cross-polarization and the well-resolved character of the spectra to the formation of a phase that has an organized columnar structure and a high molecular mobility. It is thought that the Pc molecules rotate rapidly around the columnar axes. Evidence for this interpretation comes from the determination of the chemical shift anisotropy by using Herzfeld's and Berger's spinning side band analysis.[25] Table 4 shows the chemical shift tensor (CST) obtained for the C4 atom of (*S*)-Pc(8,2) at different temperatures. At elevated temperatures the principal values σ_{11} and σ_{22} of this tensor, which lie in the plane of the molecule, are equal; this demonstrates that the system has axial symmetry. At low temperatures the tensor is clearly nonaxial. This averaging of the chemical shift anisotropy in the plane of the molecule when entering the mesophase was also observed for Pc(12).

0570-0833/95/0303-0174 $ 30.00+.25/0 Chem. Eur. J. 1995, 1, No. 3

Table 4. Principal values of the chemical shift tensor of the C4 carbon of (*S*)-Pc(8,2) at various temperatures [a].

T/°C	σ_{11}	σ_{22}	σ_{33}
180	184	184	75
155	182	182	76
−15	210	162	61
−60	211	161	60

[a] The σ_{11}, σ_{22} axes are parallel with the molecular plane; the σ_{33} axis is perpendicular to this plane.

Side-chain signals: The linear chain phthalocyanine Pc(11) shows a sudden change in the high field (alkane) region of the solid state NMR spectrum around the K → D_h transition temperature, as we reported previously.[9] Broad peaks are observed in the crystalline phase; this indicates that the side chains are rigid. In the mesophase they appear liquidlike (sharp lines). A similar behavior was observed for Pc(12). Such a sudden change did not occur in the case of (*S*)-Pc(8,2). The lines were also broad below 0 °C (Fig. 3a) and sharp above 85 °C (Fig. 3c),

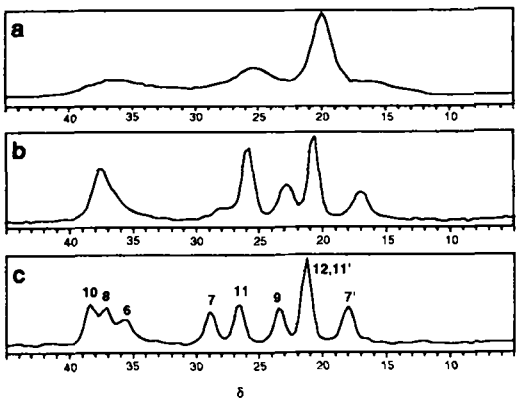

Fig. 3. Aliphatic regions of the solid-state ^{13}C NMR spectra of (*S*)-Pc(8,2) a) at −60 °C with cross-polarization, b) at 25 °C with cross-polarization, and c) at 115 °C with direct pulse excitation.

but—in contrast to Pc(11) and Pc(12)—the peak widths changed gradually in between these two temperatures. Very striking is the observation that the temperature at which each side-chain carbon atom of (*S*)-Pc(8,2) becomes mobile increases with decreasing distance of the atom from the core, which was not so clearly observed for the linear-chain Pcs. The signals of the three terminal carbon atoms C11, C11′ and C12 of (*S*)-Pc(8,2) were already sharp at −30 °C; this suggests that this section of the side chains is mobile at this temperature. Above 10 °C the peaks of atoms C7′, C9, and C10 became sharper (Fig. 3b), and above 60 °C the mobility of atoms C7 and C8 increases. Finally, atom C6 became mobile above 85 °C. A similar stepwise change in side-chain mobility was found by Leisen et al. in their NMR studies of a liquid-crystalline triphenylene.[26]

The signals of the side-chain carbon atoms in the solid-state spectrum at different temperatures are summarized in Table 3. They are shifted upfield relative to those in the solution spectrum. This effect is most pronounced for carbon atoms C5 and C7′, especially at lower temperatures. This result provides information about the conformation of the side chains of the phthalocyanines. It is known that a γ-substituent shields a carbon atom, causing a shift of 5 ppm, when it is in a gauche conformation with respect to this carbon atom.[27] The side-chain conformation that is consistent with a γ-effect on both C5 and C7′—and only on these carbon atoms—is shown in Figure 4a. The other possible conformations (Fig. 4b,c) are unlikely as these would lead to an upfield shift on carbon atom C8. Assuming the most stable arrangement for C5 (in-plane with the Pc core and C5–O *syn* to C3–C4 of the aromatic ring),[7, 26] we derived the conformation adopted by the side chains, at least at temperatures below 60 °C (Fig. 4d). Thus, the methyl groups at the chiral centers are positioned alternately above and below the molecular plane. Such an arrangement may result in an overall chiral molecular shape, which could be the origin of the helical superstructure in the D_h^* phase.

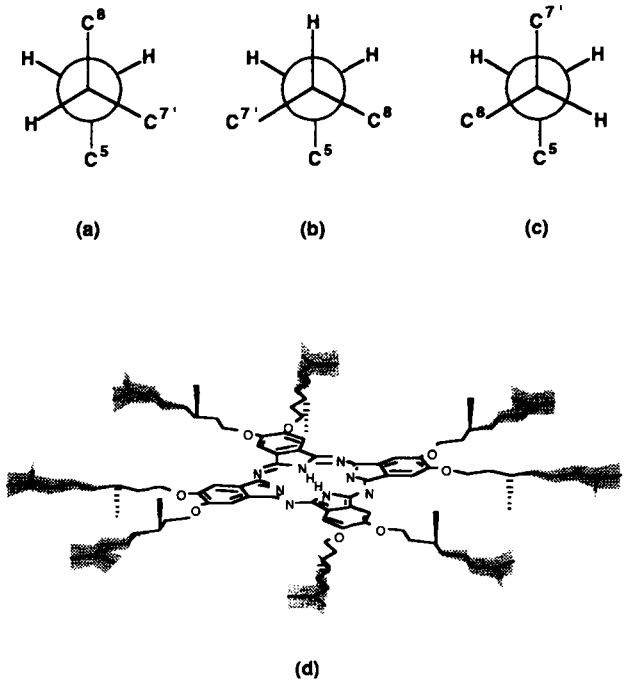

Fig. 4. Newman representation of the three possible side-chain conformations of (*S*)-Pc(8,2) around the bond between C6 and C7 (a–c), and representation of the most probable molecular conformation of the phthalocyanine (d). The ends of the side chains have no fixed conformation (shaded areas).

Proton spectra: The solid state ^1H NMR spectrum of Pc(12) in its mesophase displayed three peaks (not shown): a large one at $\delta = 1.5$ resulting from the side chain protons, a small peak at $\delta = 4.1$ from the protons at C5, and a peak at $\delta = 5.8$ from the aromatic protons. The latter is shifted 3 ppm upfield relative to the corresponding peak in the solution spectrum, because of intermolecular ring current effects.[9] On cooling line broadening was found to take place at the transition to the crystalline phase near 85 °C, probably because the axial symmetry phases out. This change takes place within a temperature range of 5 °C. A similar line broadening of the proton signals was observed on cooling (*S*)-Pc(8,2) (results not shown). However, with the latter compound this change took place over a larger temperature range (82–70 °C); this is consistent with the DSC data.

Luminescence: Energy migration in the columns of (*S*)-Pc(8,2) and (*R*,*S*)-Pc(8,2) was studied by means of luminescence experiments in the temperature range of 4–400 K. Blasse et al. have performed similar experiments with the phthalocyanine Pc(12) containing linear side chains.[10b] They discussed their results in

terms of a model in which mobile excitons decay, after excitation in the Q band, at different sites in the columnar stacks, namely, intrinsic sites (positionally undisturbed Pc molecules, radiative decay), extrinsic sites (strongly disturbed molecules, radiative decay), and quenching sites (nonradiative decay). The wavelengths of emission were reported to be 795 nm for the intrinsic sites and approximately 820 nm for the extrinsic sites.

Luminescence spectra of (*S*)-Pc(8,2) and (*R,S*)-Pc(8,2) were recorded during a heating and cooling cycle starting at 4 K. A selection of spectra of (*S*)-Pc(8,2) at different temperatures are given in Figure 5. Figure 6 shows the intensity at the wavelength

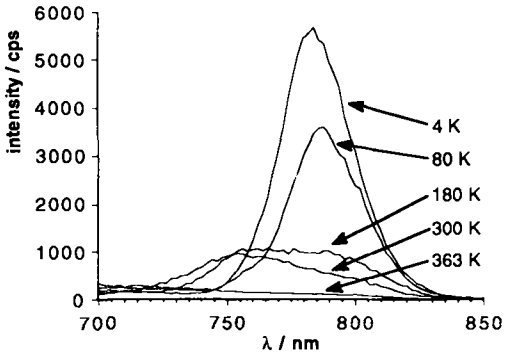

Fig. 5. Emission spectra of (*S*)-Pc(8,2) at different temperatures. Excitation is in the Q band at 560 nm.

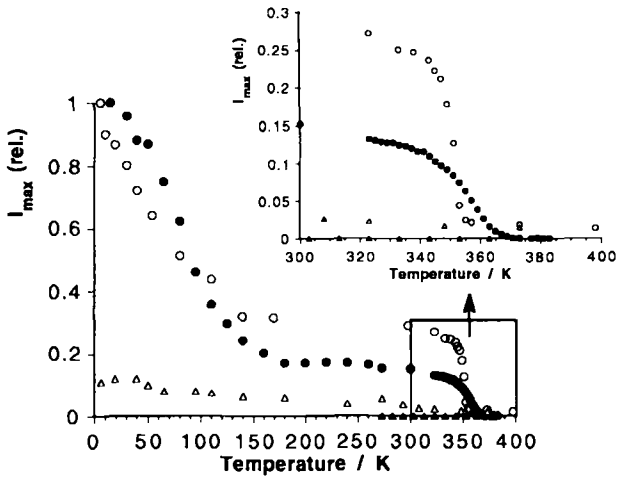

Fig. 6. Normalized emission intensity at the wavelength of maximum emission measured for (*R,S*)-Pc(8,2) during heating (○) and cooling (△) and for (*S*)-Pc(8,2) during heating (●) and cooling (▲). Inset: enlargement of the temperature range 300–400 K.

of the emission maximum (I_{max}) as a function of temperature for the two compounds. The intensity is seen to decrease gradually with increasing temperature until a plateau is reached at approximately 200 K. This loss in intensity was also observed for Pc(12), and can be explained by the fact that excitons migrate faster through the stacks at higher temperatures and can reach quenching sites (copper phthalocyanine molecules left from the synthesis) more easily. At around 345 K, the luminescence drops to almost zero for both (*S*)-Pc(8,2) and (*R,S*)-Pc(8,2). In the case of the latter compound this sudden change in intensity coincides with the K → D_h transition; it occurs within a temperature range of 10 °C. This behavior is similar to that found for Pc(12). In the mesophase—unlike the crystalline phase—the Pc molecules are oriented perpendicular to the columnar axes; this allows a faster migration of the excitons and a more rapid trapping at quenching sites.[10b] The drop in luminescence intensity observed for (*S*)-Pc(8,2) cannot be due to a K → D_h transition, because such a transition is not observed by DSC. Moreover, the disappearance of the luminescence is much slower for (*S*)-Pc(8,2) than for (*R,S*)-Pc(8,2), as it occurs over a temperature range of around 25 °C. Although it does not coincide exactly, this change may be related to the slow transition between 45 and 65 °C found by DSC. The latter probably involves the transformation of a distorted columnar mesophase to an undistorted one. In the undistorted phase energy migration will be more efficient. Other experiments corroborate this hypothesis (see below).

For both (*S*)-Pc(8,2) and (*R,S*)-Pc(8,2) the initial emission intensity does not reappear on cooling, even at 4 K. Apparently, the mesophase is frozen at low temperatures, and fast exciton migration can still occur through the well-organized, stacked Pc cores. We observed a similar fast energy migration at low temperatures for phthalocyanines in which the mesophase was fixed by polymerization.[28]

Phthalocyanine (*S*)-Pc(8,2) differs in an interesting way from (*R,S*)-Pc(8,2) and Pc(12). For the latter two compounds a gradual shift in the wavelength of the emission maximum was observed with increasing temperature, from around 790 nm at 4 K to around 820 nm above 80 K. This phenomenon was explained previously by a change in the radiative decay mechanism from a decay through intrinsic sites to decay through extrinsic sites.[10b] The emission of (*S*)-Pc(8,2) was found to shift to shorter wavelengths with increasing temperature, from 788 nm at 4 K to 756 nm above 200 K (Fig. 5). This contrasting behavior must be due to the helical columnar structure of (*S*)-Pc(8,2). At low temperatures (*R,S*)-Pc(8,2) and Pc(12) are crystalline, whereas (*S*)-Pc(8,2) is probably in a distorted helical mesophase, that is, the molecules are more or less cofacially stacked, but the length of the columns is limited. At 4 K fast energy migration is therefore still possible for (*S*)-Pc(8,2), but trapping takes place more frequently at the large number of distorted (extrinsic) sites. On increasing the temperature, thermal detrapping occurs, and emission from the undistorted (intrinsic) sites at shorter wavelength is now predominant. Above 70 °C the columnar stacking improves slowly, and energy migration to quenching sites is so efficient that only nonradiative quenching takes place.

Microwave Conductivity: In a previous paper we discussed the effect of structural modifications on charge migration, as measured by the TRMC technique, in several mesogenic Pcs.[11i] The results obtained with (*S*)-Pc(8,2) and (*R,S*)-Pc(8,2) are summarized in this section.

Figure 7 shows the temperature dependence of the dose-normalized end-of-pulse conductivity ($\Delta\sigma_{eop}/D$) of the two phthalocyanines. The initial value of $\Delta\sigma_{eop}/D$ measured in the crystalline phase of (*R,S*)-Pc(8,2) at 25 °C is close to that found in the crystalline phase of *n*-alkoxy Pcs.[11i] The sudden decrease of the conductivity by a factor of 5 at the K → D_h transition is also observed with *n*-alkoxy Pcs. It is ascribed to the fact that the molecular motions in the mesophase are stronger than in the crystalline phase; this makes the path for charge migration less efficient.[11i] On cooling $\Delta\sigma_{eop}/D$ of (*R,S*)-Pc(8,2) does not immediately return to its initial value, as found for the *n*-alkoxy compounds. This feature is consistent with the absence of a D_h → K phase transition in the DSC cooling runs. The conductivity eventually returns, however, to the starting level after the material is left standing at room temperature for a period of several hours. During this time it slowly reassumes the initial

0570-0833/95/0303-0176 $ 30.00+.25/0 Chem. Eur. J. 1995, 1, No. 3

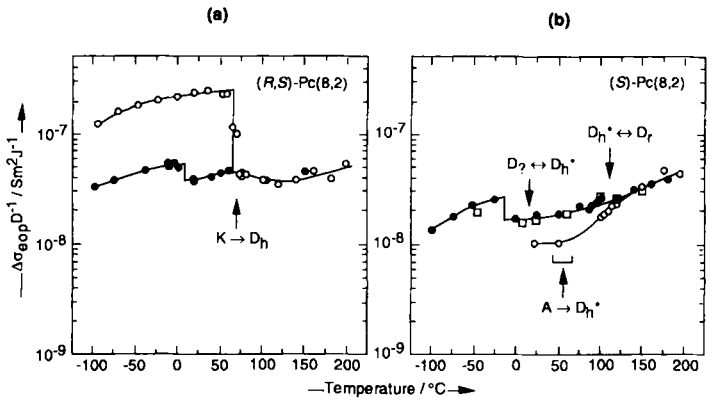

Fig. 7. Dose-normalized radiation-induced end-of-pulse conductivity vs. temperature for a) (*R*,*S*)-Pc(8,2) and b) (*S*)-Pc(8,2) on heating (o) and cooling (•). For (*S*)-Pc(8,2) the open squares represent the values during the second heating. The arrows indicate the phase-transition temperatures.

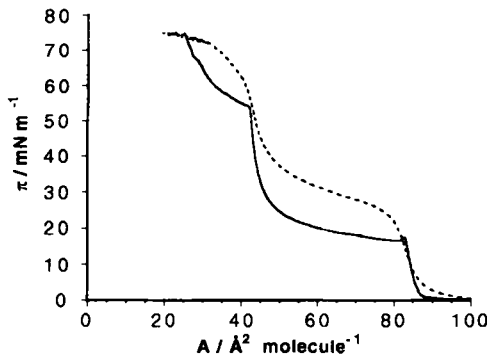

Fig. 8. Surface pressure vs. surface area isotherms for (*R*,*S*)-Pc(8,2) (broken line) and (*S*)-Pc(8,2) (solid line) at a subphase temperature of 20 °C.

solid-state structure. The small increase in $\Delta\sigma_{eop}/D$ observed at around 0 °C, is probably the result of a phase transition that is not seen by DSC.

In contrast to the mixture of stereoisomers, (*S*)-Pc(8,2) does not show a sudden decrease in $\Delta\sigma_{eop}/D$ on heating; this is in agreement with the absence of a K → D_h transition for the latter compound. Remarkably, the $D_h^* \rightarrow D_r$ transition at 111 °C has no influence on the charge migration. Above 150 °C both (*S*)-Pc(8,2) and (*R*,*S*)-Pc(8,2) have the same $\Delta\sigma_{eop}/D$ value. Figure 7b shows that, on cooling, the conductivity of the optically active phthalocyanine does not return to its starting value, but remains approximately twice as high. This result suggests that the stacking of the molecules in a sample of (*S*)-Pc(8,2) that is freshly precipitated from solution is unfavorable for charge migration, and that this stacking improves irreversibly on heating. The same conclusion was drawn from the energy migration experiments. This observation corroborates the idea (see above) that the irreversible endothermic peak observed by DSC between 45 and 65 °C is not a real phase transition but a slow reorganization of the phthalocyanine molecules.

On further cooling, (*S*)-Pc(8,2) displayed a slight increase in $\Delta\sigma_{eop}/D$ at approximately 0 °C, which coincides with the phase transition found by DSC. A second heating trajectory was found to correspond with the first cooling trajectory (see Fig. 7b). The low starting value recorded for the freshly precipitated sample at room temperature was never observed again after the first heating trajectory.

The values of $\Delta\sigma_{eop}/D$ of (*S*)-Pc(8,2) below 150 °C are lower than those of (*R*,*S*)-Pc(8,2). This indicates that the molecular packing in the former compound is less favorable for one-dimensional charge migration than in the latter. We will return to this subject below.

Monolayers and LB Films: The construction of LB films from discotic molecules that are liquid crystalline at room temperature has not been reported in the literature. Because such liquid-crystalline behavior is thought to be favorable for the construction of well-organized and stable LB films,[29] we performed monolayer studies on (*S*)-Pc(8,2).[30]

Figure 8 shows the pressure–area isotherms for (*R*,*S*)-Pc(8,2) and (*S*)-Pc(8,2) at 20 °C. The two isotherms are very similar and indicate that phase transitions occur when the films are compressed. For (*S*)-Pc(8,2) a first rise in surface pressure is found at an area of 85 Å^2 per molecule. This small number suggests that the planes of the phthalocyanine molecules are oriented perpendicular to the water surface. Four side chains are bent towards the air–water interface, while the other side chains extend into the air. Similar values of the molecular areas have been reported for other phthalocyanines.[31] On further lowering the surface area, a second pressure increase can be seen at 45 Å^2 per molecule. Interestingly, this value is approximately half the value of the area where the first increase takes place; this suggests that a bilayer is formed (see also below). At higher subphase temperatures even a third rise in pressure (not shown) was observed at one third of the area of the first increase, which may point to the formation of a triple layer.

Stability is a prerequisite if one wants to transfer a monolayer uniformly onto a substrate. We therefore studied the change in surface area as a function of time when the surface pressure was kept constant. The decays of the surface area per hour for (*S*)-Pc(8,2) at various surface pressures and temperatures are reported in Table 5. At a surface pressure of 8 mN m^{-1} the monolayer was only reasonably stable at low temperatures. In contrast, at a surface pressure of 30 mN m^{-1}, that is, when a bilayer is probably present, a stable film was obtained at 20 °C. This holds for both (*S*)-Pc(8,2) and (*R*,*S*)-Pc(8,2).

Table 5. Decay of the surface area of (*S*)-Pc(8,2) films at the air–water interface as a function of the surface pressure (π) and the temperature.

π/mN m^{-1}	*T*/°C	decay/Å^2 molecule^{-1} h^{-1}
8	5	0.966
8	35	2.66
30	20	0.298

Transfer of the (*S*)-Pc(8,2) film turned out to be very irregular and troublesome in the monolayer phase, even at lower temperatures. However, in the bilayer phase transfer was possible with a constant transfer ratio close to unity (Fig. 9). Transfer was observed during both upstroke and downstroke dipping, that is, Y-type multilayers were obtained. Up to 20 bilayers were assembled onto hydrophobized glass, quartz, silicon, gold, and zinc sulfide substrates.

The anisotropy of the LB films was clearly visible by polarizing microscopy. When a glass substrate containing 10 bilayers was placed between crossed polarizers no light was transmitted when the transfer direction of the LB film was parallel to the analyzer or polarizer. Intermediate orientations of the glass gave a structureless bright field. The anisotropic properties of the material were studied by polarized absorption spectroscopy on quartz slides with 10 bilayers on both sides of the substrate.

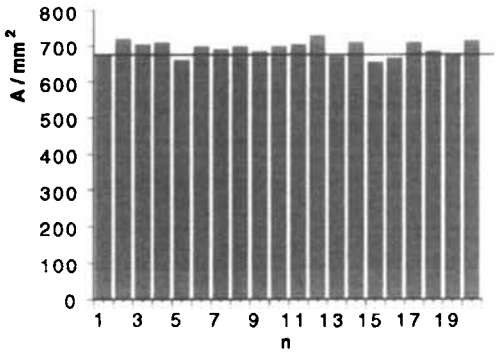

Fig. 9. Transferred area vs. layer number measured for the deposition of a bilayer of (*S*)-Pc(8,2) on a gold substrate at a surface pressure of 30 mN m^{-1} and a temperature of 20 °C. The first layer is from downstroke deposition. The horizontal line indicates the covered area on the substrate.

Figure 10 shows the absorption spectra of a freshly prepared film and those of the same film after annealing for one hour at 100 °C, with the light polarized parallel and perpendicular to the transfer direction. For the freshly prepared sample the maximum of the *Q* band is found at a wavelength of 617 nm. The blue-shift of this band relative to that in the solution spectrum

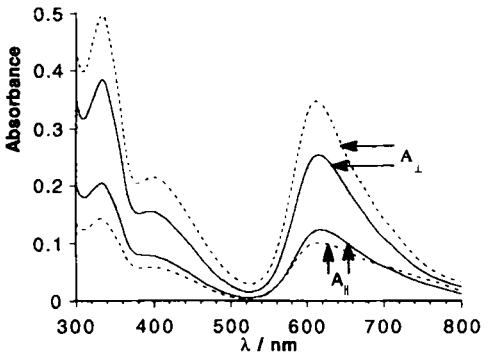

Fig. 10. Electronic absorption spectra of 2 × 10 bilayers of (*S*)-Pc(8,2) on quartz slides directly after preparation of the LB films (solid lines) and after 15 h annealing at 100 °C (broken lines). The spectra were recorded with the light polarized parallel (∥) and perpendicular (⊥) to the dipping direction.

indicates that the molecules in the LB film are stacked in columns; the spectrum is similar to those of alkoxymethyl Pc and of alkoxy Pc in their mesophases.[10c, 32] The wavelength of the absorption maximum decreases to 612 nm after annealing of the film, which suggests that the number of molecules in the stacks has increased. The highest absorption is found when the light is polarized perpendicular to the transfer direction, which means that the columns are predominantly aligned in the dipping direction. The dichroic ratio (*R*) can be determined by means of Equation (5),[33] where $(A_\perp)_i$ and $(A_\parallel)_i$ are the absorp-

$$(A_\perp)_i = R(A_\parallel)_i + (a - Rb) \tag{5}$$

tions measured at the *i*th wavenumber based on the given baselines, and *a* and *b* are the differences between the given baselines and the true baseline. Table 6 shows the values of *R* that were calculated by fitting the datapoints to Equation (5). A dichroic ratio of 1.85 was found for the freshly prepared film, and a value of 3.32 for the film that had been annealed for one hour. Longer annealing times did not further increase this number. The two-dimensional order parameter (*S*) for the cofacial stacks and the

Table 6. Dichroic ratio (*R*), two dimensional order parameter (*S*), mean deviation angle (ψ), and real (n_r) and imaginary (n_{im}) parts of the refractive index, both parallel and perpendicular to the transfer direction, of an LB film of (*S*)-Pc(8,2) before and after annealing for one hour at 100 °C [a].

	Before annealing	After annealing
R	1.85	3.32
S	0.29	0.54
ψ/°	36	29
$n_{r,\parallel}$	1.68	1.63
$n_{r,\perp}$	1.78	1.83
$n_{im,\parallel}$	0.02	0.01
$n_{im,\perp}$	0.08	0.08

[a] The refractive indices are derived from ellipsometry measurements, the other parameters are obtained from spectroscopic studies.

mean deviation angle of the columnar axis from the transfer direction (ψ) can be calculated from Equations (6) and (7).[34] As can be seen in Table 6, *S* increases and ψ decreases on thermal annealing; this clearly demonstrates the beneficial effect of this treatment on the organization of the molecules in the LB films.

$$S = \frac{R-1}{R+1} \tag{6}$$

$$\langle \sin^2\psi \rangle = \frac{1}{R+1} \tag{7}$$

In the LB trough the molecules of (*S*)-Pc(8,2) are probably oriented perpendicular to the water surface; the same also holds for the bilayer phase at a surface pressure of 30 mN m^{-1}. FT-IR spectroscopy revealed that this molecular orientation is retained in the transferred LB films (results not shown). The out-of-plane vibrations at 850 (=C–H) and 740 cm^{-1} (Pc ring deformation) are practically absent in the grazing incidence reflection (GIR) spectrum (the field vector of the IR beam is oriented perpendicular to the substrate surface), whereas they are very distinct in the transmission (TM) spectrum when the field vector is parallel to the transfer direction. In the TM spectrum recorded with the polarized light perpendicular to the transfer direction, these out-of-plane vibrations are only weak. This difference in the two TM spectra is due to the anisotropic arrangement of the molecules within the layers. The perpendicular orientation of the Pc molecular planes with respect to the substrate surface did not change after thermal annealing of the film.

In order to confirm the presence of bilayers, ellipsometry experiments were carried out on LB films deposited on a silicon substrate. The ellipsometric parameters Δ and Ψ were measured for parallel and perpendicular orientations of the sample with respect to the plane of incidence of the laser beam. These values were fitted with an anisotropic model,[35] in such a way that the thickness of the film was equal for both orientations. The calculated film thicknesses as a function of the number of tranferred layers are displayed in Figure 11. From this Figure a layer thickness of 60.4 Å can be derived. This high value can only be explained by a transfer of bilayers onto the substrate: half the thickness is close to the diameter of one molecule (31.63 Å) as derived from X-ray measurements (Table 2). Thermal annealing did not affect the film thickness within experimental error, but the real and imaginary refractive indices became more anisotropic, as can be judged from the values in Table 6.

The layer structure of the film was studied by small-angle X-ray scattering measurements on a sample containing 10 bilay-

0570-0833/95/0303-0178 $ 30.00+.25/0 Chem. Eur. J. 1995, 1, No. 3

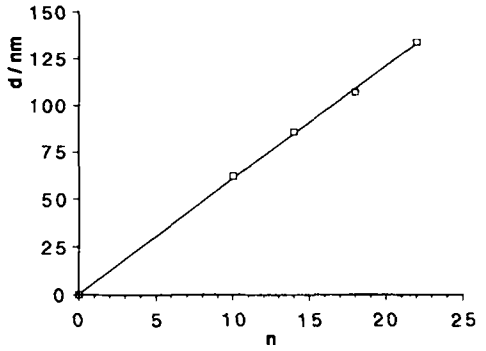

Fig. 11. Film thicknesses, as calculated from ellipsometry measurements, vs. the number of transferred bilayers of (*S*)-Pc(8,2). The measurements indicated that a 6 nm SiO_2 layer was present on the bare silicon substrate. The measured values are corrected for this 6 nm layer.

ers of (*S*)-Pc(8,2) on a glass slide. As can be seen in Figure 12, the scattering curve of the freshly prepared sample at 20 °C shows three broad peaks, which correspond to *d* spacings of 31.9, 25.5, and 21.1 Å. It is not possible to derive an unequivocal structure from this result. The 31.9 and 25.5 Å spacings may be related to a rectangular and a hexagonal arrangement of the cylindrical columns, respectively. The latter spacing is approximately equal to the (1000) reflection of the bulk sample (Table 2). Both arrangements are probably present in the film. The 21.1 Å spacing might be some higher order reflection. Alternatively, there could be a coexistence of different phases probably with different orientations. The film would then consist of domains with different structures and lattice periodicities. This is consistent with the low number of Kiessig fringes at small angles, which indicates that the overall film thickness is not well defined.

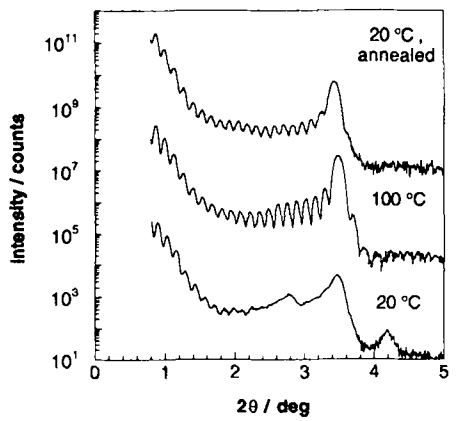

Fig. 12. X-ray scattering curves at different temperatures of a sample containing 10 bilayers of (*S*)-Pc(8,2) on glass. The curves are displaced along the *y* axis to avoid overlapping.

When the film is heated to 100 °C, only one of the Bragg peaks remains, namely, the one at 25.4 Å (Fig. 12). Moreover, the number of Kiessig fringes increases, as a result of a decrease in roughness of the film surface. It can be concluded that a reorganization has taken place to a hexagonal packing. At the same time the thickness of the film has become more homogeneous. From the periodicity of the Kiessig fringes the overall film thickness can be calculated to be 659 Å. This value is not equal to the product of the layer spacing and the number of layers (20 × 25.4 = 508 Å). The molecular area of the film at the air–water interface and the constant and well-defined transfer ratio (see above) indicate that bilayers must have been deposited. It is possible that the bilayers rearrange on the solid support, a process which leads to a thicker film with defects. It is also conceivable that only parts of the film are responsible for the Kiessig fringes, which might fail to give a Bragg reflection owing to a disordered structure. More experiments are required to solve this problem. The overall film thickness calculated from ellipsometry (604 Å) deviates somewhat from the X-ray results (659 Å); the discrepancy is due to the larger inaccuracy of the former technique.

When the film was cooled back to 20 °C its structure remained unchanged, even after a period of 10 days (Fig. 12). The layer spacing was found to increase slightly to 25.8 Å.

Circular Dichroism: Circular dichroism (CD) spectroscopy is a powerfull tool for obtaining structural information related to optical activity.[21] We studied phthalocyanine (*S*)-Pc(8,2) with the help of this technique. Spectra were recorded in solution and of LB films.

A solution of (*S*)-Pc(8,2) in chloroform did not give a CD spectrum. A similar negative result was obtained in the case of a freshly prepared LB film. However, when the temperature was raised above 60 °C this film displayed CD activity (Fig. 13).

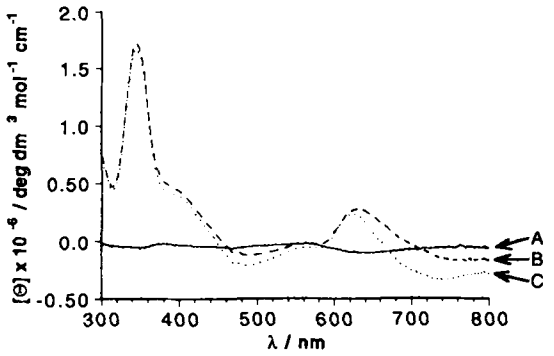

Fig. 13. Circular dichroism spectra of 2 × 10 bilayers of (*S*)-Pc(8,2) on quartz: A) freshly prepared sample at 20 °C; B) sample at 100 °C, and C) sample after cooling to 20 °C.

When the sample was subsequently cooled to room temperature, this activity was retained, even after standing overnight. Further cooling down to −10 °C did not change the spectrum. The calculated molecular ellipticity [θ] is very high. Under the same experimental conditions an LB film of (*R*,*S*)-Pc(8,2) did not show any CD activity at room temperature or at elevated temperatures. Apparently, the thermal annealing of the LB film of (*S*)-Pc(8,2) leads to a more ordered structure (as discussed above) and consequently to the observed strong CD activity. As a solution of (*S*)-Pc(8,2) does not give a CD spectrum, the CD activity of the film must be the result of a chiral superstructure.

When measuring the CD spectrum of an anisotropic solid medium, one should be aware of artifacts due to linear dichroism (LD).[36] A method to check for such effects is to record spectra at sample orientations differing by 90°.[37] We observed no appreciable difference when the LB film of (*S*)-Pc(8,2) was measured in horizontal or vertical position. Another argument against a LD contribution in our CD spectra is the absence of CD activity in the freshly prepared LB film of (*S*)-Pc(8,2) and in the film of (*R*,*S*)-Pc(8,2), although LD was clearly observed in the two samples.

Figure 13 clearly shows a negative exciton effect in the *Q*-band region, especially for the sample that was cooled to 20 °C after annealing. This feature indicates that the $\pi-\pi^*$ transition dipoles of the Pc molecules are coupled in a left-handed chiral arrangement.[21] It is possible to derive the exact orientations of the molecules with respect to each other by comparing the measured CD spectrum with the calculated one, but because of the complexity of the system this is not easily performed. We plan to do CD calculations in the near future.

Discussion

From the results presented in the foregoing section a rather complete picture emerges of the structure and dynamic properties of optically active phthalocyanine (*S*)-Pc(8,2) in its various phases. One of the striking results is that this compound lacks a crystalline phase, in contrast to (*R,S*)-Pc(8,2). This was not expected a priori. Because (*S*)-Pc(8,2) is stereoisomerically pure, it was thought that it would crystallize more readily than the mixture of (*R,S*)-Pc(8,2), which contains 43 stereoisomers. Why this is not the case is not yet clear.

A freshly precipitated sample of (*S*)-Pc(8,2) is in a kind of distorted mesophase, which slowly reorganizes to a more ordered mesophase on heating above 65 °C. This reorganization—which is irreversible—is evident from the following experimental results: (i) the DSC runs, which show a broad peak with a low transition enthalpy in the first heating scan only, (ii) the disappearance of luminescence, indicating that energy migration is very efficient in the more ordered mesophase, (iii) an increase of the microwave conductivity, (iv) the improvement of the anisotropy and the layer structure of the LB films of the compound, and (v) the development of a very strong CD activity in the LB films. The difference between the distorted mesophase in the freshly precipitated sample and the ordered mesophase after annealing may be the number of kinks in the columnar stacks, which is probably larger in the former than in the latter. This can be concluded from luminescence experiments, which show that in freshly precipitated (*S*)-Pc(8,2) at low temperatures energy trapping predominantly occurs at extrinsic sites.

The ordered mesophase of (*S*)-Pc(8,2) has a unique structure. From X-ray diffraction experiments, polarization microscopy, and CD measurements we conclude that a chiral superstructure is present in this phase. Three possible limiting structures are shown in Figure 14. Destrade et al. postulated the presence of a spiral staircaselike structure in the mesophase of an optically active triphenylene, where the molecules are displaced perpendicular to the columnar axis (Fig. 14A).[22] Such a molecular arrangement is unlikely for (*S*)-Pc(8,2) since it would lead to an intercolumnar distance that is larger than the distance between the columns in the mesophase of (*R,S*)-Pc(8,2). Our X-ray results show that the intercolumnar distance of (*S*)-Pc(8,2) is slightly smaller than that of (*R,S*)-Pc(8,2) (Table 2). Levelut et al. proposed that the above-mentioned chiral triphenylene molecules are aligned in a way as is shown in Figure 14B:[16] along the columnar axis, the staggering angle of two neighboring molecules is constant and always in the same direction. In our case such a superstructure could result in the dipoles of the aromatic cores of the Pc molecules being arranged in the form of a left-handed helix and give a negative CD effect. It is, however, difficult to conceive how such a staggered arrangement could give rise to the characteristic X-ray diffraction pattern shown in Table 2. We therefore propose a third superstructure, which is schematically represented in Figure 14C. The molecules of (*S*)-Pc(8,2) are slightly tilted and, along the columnar axis, the normal of the Pc-plane gradually rotates around the columnar axis forming a left-handed helix. We denote this novel mesophase as a D_h^* phase. The columnar modulation giving rise to the X-ray diffraction pattern is now more obvious. CD calculations and X-ray diffraction studies as well as NMR experiments on aligned samples will give more conclusive information about the actual structure. Such experiments are under way.

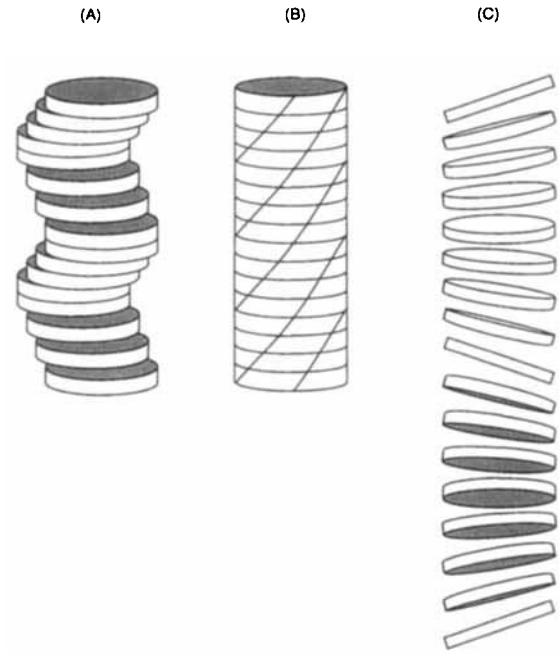

Fig. 14. Schematic representation of the three possible helical arrangements of the columns in the D_h^* phase of (*S*)-Pc(8,2).

No solid-state NMR signals from the aromatic cores of the Pc molecules are observed in the D_h^* phase, probably because of line broadening due to the helical displacement of the Pc macrocycles and because of exchange broadening due to molecular motions. The mobility of the side chains increases gradually with increasing temperature. From the signals in the NMR spectra it follows that the side chains adopt an overall chiral molecular conformation, as illustrated in Figure 4, at least at temperatures below 60 °C. The presence of such a chiral conformation may be the reason why a helix is formed. The helical distortion of the columns appears to be unfavorable for intracolumnar charge migration. This can be concluded from the fact that a lower microwave conductivity is observed at room temperature for (*S*)-Pc(8,2) than for (*R,S*)-Pc(8,2).

On heating (*S*)-Pc(8,2) from the D_h^* phase a small transition is observed by DSC at 111 °C. The hexagonal arrangement of the columns is lost and a new phase appears, probably a D_r phase. A dramatic change near this phase transition is recorded by solid-state ^{13}C NMR: the Pc molecules start to rotate around their columnar axes and the side chains become completely liquidlike. Interestingly, these changes have hardly any influence on the charge migration, as the microwave conductivity shows no sudden change around this transition. The reverse transition from the D_r to the D_h^* phase appears to be slow, according to DSC and solid-state ^1H NMR.

On cooling (*S*)-Pc(8,2) from the D_h^* phase another transition occurs at 3 °C. The precise structure of the new phase could not be elucidated. The transition enthalpy is very low, which suggests that no major structural change takes place. NMR measurements indicate that the aromatic core as well as the side

© VCH Verlagsgesellschaft mbH, D-69451 Weinheim, 1995 0570-0833/95/0303-0180 $ 30.00+.25/0 Chem. Eur. J. 1995, 1, No. 3

chains of the Pc molecules become almost completely immobile on the NMR time scale below 3 °C. TRMC measurements reveal a slight increase in the microwave conductivity. We believe that at $T < 3$ °C, the structure of the D_h^* phase becomes frozen, which results in a slightly better intracolumnar charge migration. The columnar stacking is not changed, since energy migration remains very efficient and the CD activity is still present.

Our experiments indicate that intracolumnar charge migration is faster in the crystalline phase than in the mesophase. Apparently, transport of electrons and electron holes is very much dependent on the molecular motions that occur in the mesophase and on the columnar deformations that are present (columnar kinks and helical superstructure). Even in the supercooled, frozen mesophase charges do not migrate very efficiently. On the contrary, energy migration appears to be faster in the mesophase than in the crystalline phase and is not affected by molecular motions. It is disfavored by the noncofacial stacking of the molecules in the crystalline phase and by columnar kinks in the mesophase. For efficient energy migration, close contact, whether permanent or incidental, between the molecules in one column seems to be essential. For hopping of electrons or holes, an undistorted, rigid stacking is required.

We have shown that it is possible to prepare an excellent quality LB film from our mesogenic Pc.[38] Very striking is the observation that a bilayer, and perhaps even a multilayer, of (*S*)-Pc(8,2) can be formed at the air–water interface. The bilayer is more stable and can be better transferred than the monolayer. So far, only few examples are known of compounds that form multilayers on a water surface.[39] Rapp et al. described a smectic liquid crystal displaying this behavior.[39b] Multilayer formation was explained from the fact that (i) the mesogens have only weak interactions with the water surface and (ii) they do not collapse to an undefined state, but rather form highly ordered structures, guided by the interactions between the molecules in the liquid-crystalline phase. In a similar way, the formation of stable bilayers by (*S*)-Pc(8,2) (and also by (*R,S*)-Pc(8,2)) can be explained from the occurrence of a mesophase at ambient temperature.

The ability to form well-organized LB films, the rich phase behavior, and the optically active properties make (*S*)-Pc(8,2) an interesting compound for future applications, for example, in electronic and ferroelectrical devices, and in optical data storage systems.

Acknowledgements: We would like to thank G. H. Nachtegaal, J. W. M. van Os, and H. Janssen (National HF NMR Facility, University of Nijmegen) for their technical assistance with the NMR measurements, R. van Puijenbroek (Akzo Nobel, Arnhem) for powder X-ray diffraction measurements, and M. N. Teerenstra (University of Groningen) for his assistance with the LB experiments. H. P. J. M. Dekkers (University of Leiden, The Netherlands) is acknowledged for useful discussions about the CD experiments. This research was supported financially by the Dutch Innovation Oriented Research Programme (IOP) of the Ministry of Economic Affairs.

Received: November 14, 1994 [F18]

[1] S. Chandrasekhar, B. K. Sadashiva, K. A. Suresh, *Pramana* **1977**, *9*, 471.
[2] For a recent review see: S. Chandrasekhar, G. S. Ranganath, *Rep. Prog. Phys.* **1990**, *53*, 57.
[3] C. C. Leznoff, A. B. P. Lever, *Phthalocyanines, Properties and Applications, Vol. 1–3*; VCH, New York, **1989–1993**.
[4] C. Piechocki, J. Simon, A. Skoulios, D. Guillon, P. Weber, *J. Am. Chem. Soc.* **1982**, *104*, 5245.
[5] a) M. J. Cook, S. J. Cracknell, K. J. Harrison, *J. Mater. Chem.* **1991**, *1*, 703; b) A. N. Cammidge, M. J. Cook, K. J. Harrison, N. B. McKeown, *J. Chem. Soc. Perkin Trans. 1* **1991**, 3053; c) M. K. Engel, P. Bassoul, L. Bosio, H. Lehmann, M. Hanack, J. Simon, *Liq. Cryst.* **1993**, *15*, 709; d) M. Hanack, A. Beck, H. Lehmann, *Synthesis* **1987**, 703; e) I. Cho, Y. Lim, *Mol. Cryst. Liq. Cryst.* **1988**, *154*, 9; f) J. F. van der Pol, E. Neeleman, J. W. Zwikker, R. J. M. Nolte, W. Drenth, J. Aerts, R. Visser, S. J. Picken, *Liq. Cryst.* **1989**, *6*, 577; g) W. T. Ford, L. Sumner, W. Zhu, Y. H. Chang, P.-J. Um, K. H. Choi, P. A. Heiney, N. C. Maliszewskyj, *New J. Chem.* **1994**, *18*, 495; h) C. Piechocki, J. Simon, J.-J. André, D. Guillon, P. Petit, A. Skoulios, P. Weber, *Chem. Phys. Lett.* **1985**, *122*, 124; i) D. Lelièvre, L. Bosio, J. Simon, J.-J. André, F. Bensebaa, *J. Am. Chem. Soc.* **1992**, *114*, 4475; j) P. Doppelt, S. Huille, *New J. Chem.* **1990**, *14*, 607; k) F. Lelj, G. Morelli, G. Ricciardi, A. Roviello, A. Sirigu, *Liq. Cryst.* **1992**, *12*, 941; l) B. A. Gregg, M. A. Fox, A. J. Bard, *J. Am. Chem. Soc.* **1989**, *111*, 3024.
[6] K. Ohta, L. Jacquemin, C. Sirlin, L. Bosio, J. Simon, *New J. Chem.* **1988**, *12*, 751.
[7] J. F. van der Pol, E. Neeleman, J. W. Zwikker, R. J. M. Nolte, W. Drenth, *Recl. Trav. Chim. Pays-Bas* **1988**, *107*, 615.
[8] P. Weber, D. Guillon, A. Skoulios, *Liq. Cryst.* **1991**, *9*, 3.
[9] A. P. M. Kentgens, B. A. Markies, J. F. van der Pol, R. J. M. Nolte, *J. Am. Chem. Soc.* **1990**, *112*, 8800.
[10] a) B. Blanzat, C. Barthou, N. Tercier, J.-J. André, J. Simon, *J. Am. Chem. Soc.* **1987**, *109*, 135; b) G. Blasse, G. J. Dirksen, A. Meijerink, J. F. van der Pol, E. Neeleman, W. Drenth, *Chem. Phys. Lett.* **1989**, *154*, 420; c) D. Markovitsi, I. Lécuyer, J. Simon, *J. Phys. Chem.* **1991**, *95*, 3620.
[11] a) Z. Belarbi, C. Sirlin, J. Simon, J.-J. André, *J. Phys. Chem.* **1989**, *93*, 8105; b) Z. Belarbi, M. Maitrot, K. Ohta, J. Simon, J.-J. André, P. Petit, *Chem. Phys. Lett.* **1988**, *143* 400; c) Z. Belarbi, *J. Phys. Chem.* **1990**, *94*, 7334; d) J. F. van der Pol, M. P. de Haas, J. M. Warman, W. Drenth, *Mol. Cryst. Liq. Cryst.* **1990**, *183*, 411; e) J. F. van der Pol, M. P. de Haas, J. M. Warman, W. Drenth, *Mol. Cryst. Liq. Cryst.* **1991**, *195*, 307; f) P. G. Schouten, J. M. Warman, M. P. de Haas, J. F. van der Pol, J. W. Zwikker, *J. Am. Chem. Soc.* **1992**, *114*, 9028; g) P. G. Schouten, J. M. Warman, M. P. de Haas, M. A. Fox, H.-L. Pan, *Nature* **1991**, *353*, 736; h) J. M. Warman, M. P. de Haas, J. F. van der Pol, W. Drenth, *Chem. Phys. Lett.* **1989**, *164*, 581; i) P. G. Schouten, J. M. Warman, M. P. de Haas, C. F. van Nostrum, G. H. Gelinck, R. J. M. Nolte, M. J. Copyn, J. W. Zwikker, M. K. Engel, M. Hanack, W. T. Ford, *J. Am. Chem. Soc.* **1994**, *116*, 6880.
[12] P. G. Schouten, J. F. van der Pol, J. W. Zwikker, W. Drenth, S. J. Picken, *Mol. Cryst. Liq. Cryst.* **1991**, *195*, 291; *ibid.* **1991**, *208*, 109.
[13] D. M. Collard, C. P. Lillya, *J. Am. Chem. Soc.* **1991**, *113*, 8577.
[14] Part of this work was published as a preliminary communication: C. F. van Nostrum, A. W. Bosman, G. H. Gelinck, S. J. Picken, P. G. Schouten, J. M. Warman, A. J. Schouten, R. J. M. Nolte, *J. Chem. Soc. Chem. Commun.* **1993**, 1120.
[15] C. Destrade, N. H. Tinh, J. Malthête, J. Jacques, *Phys. Lett. A* **1980**, *79*, 189.
[16] A. M. Levelut, P. Oswald, A. Ghanem, J. Malthête, *J. Physique* **1984**, *45*, 745.
[17] M. M. Green, H. Ringsdorf, J. Wagner, R. Wüstefeld, *Angew. Chem.* **1990**, *102*, 1525; *Angew. Chem. Int. Ed. Engl.* **1990**, *29*, 1478.
[18] H. Bock, W. Helfrich, *Liq. Cryst.* **1992**, *12*, 697.
[19] N. Kobayashi, Y. Kobayashi, T. Osa, *J. Am. Chem. Soc.* **1993**, *115*, 10994.
[20] T. Arndt, C. Bubeck, A. J. Schouten, G. Wegner, *Mikrochim. Acta* **1988**, *2*, 7.
[21] N. Harada, K. Nakanishi, *Circular Dichroic Spectroscopy—Exciton Coupling in Organic Chemistry*, Oxford University Press, Oxford, **1983**.
[22] J. Malthête, J. Jacques, N. H. Tinh, C. Destrade, *Nature* **1982**, *298*, 46.
[23] a) P. M. de Wolff, *Acta Crystallogr. Sect. A* **1974**, *30*, 777; b) A. Janner, T. Janssen, *Phys. Rev. B* **1977**, *15*, 643.
[24] C. R. Safinya, N. A. Clark, K. S. Liang, W. A. Varady, L. Y. Chiang, *Mol. Cryst. Liq. Cryst.* **1985**, *123*, 205.
[25] J. Herzfeld, A. E. Berger, *J. Chem. Phys.* **1980**, *73*, 6021.
[26] J. Leisen, M. Werth, C. Boeffel, H. W. Spiess, *J. Chem. Phys.* **1992**, *97*, 3749.
[27] A. E. Tonelli, F. C. Schilling, *Acc. Chem. Res.* **1981**, *14*, 233.
[28] a) J. F. van der Pol, E. Neeleman, J. C. van Miltenburg, J. W. Zwikker, R. J. M. Nolte, W. Drenth, *Macromolecules* **1990**, *23*, 155; b) J. F. van der Pol, J. W. Zwikker, J. M. Warman, M. P. de Haas, *Recl. Trav. Chim. Pays-Bas* **1990**, *109*, 208.
[29] a) H. Ringsdorf, B. Schlarb, J. Venzmer, *Angew. Chem.* **1988**, *100*, 117; *Angew. Chem. Int. Ed. Engl.* **1988**, *27*, 113; b) T. L. Penner, J. S. Schildkraut, H. Ringsdorf, A. Schuster, *Macromolecules* **1991**, *24*, 1041; c) A. Laschewsky, *Adv. Mater.* **1989**, *1*, 392.
[30] Schutte et al. reported that (*R,S*)-Pc(8,2) can be used for deposition as LB films: W. J. Schutte, M. Sluyters-Rehbach, J. H. Sluyters, *J. Phys. Chem.* **1993**, *97*, 6069.
[31] a) C. F. van Nostrum, R. J. M. Nolte, M. A. C. Devillers, G. T. Oostergetel, M. N. Teerenstra, A. J. Schouten, *Macromolecules* **1993**, *26*, 3306; b) W. R. Barger, A. W. Snow, H. Wohltjen, N. L. Jarvis, *Thin Solid Films* **1985**, *133*, 197; c) Y. Fu, A. B. P. Lever, *J. Phys. Chem.* **1991**, *95*, 6979; d) H. Nakahara, K. Fukuda, K. Kitahara, H. Nishi, *Thin Solid Films* **1989**, *178*, 361; e) E. Orthmann, G. Wegner, *Angew. Chem.* **1986**, *98*, 1114; *Angew. Chem. Int. Ed. Engl.* **1986**, *25*, 1105; f) G. G. Roberts, M. C. Petty, S. Baker, M. T. Fowler, N. J. Thomas, *Thin Solid Films* **1985**, *132*, 113; g) Y. L. Hua, D. P. Jiang,

Z. Y. Shu, M. C. Petty, G. G. Roberts, M. M. Ahmad, *Thin Solid Films* **1990**, *192*, 383.
[32] A. W. Bosman, C. F. van Nostrum, unpublished results.
[33] S. Schwiegk, T. Vahlenkamp, Y. Xu, G. Wegner, *Macromolecules* **1992**, *25*, 2513.
[34] T. Sauer, T. Arndt, D. N. Batchelder, A. A. Kalachev, G. Wegner, *Thin Solid Films* **1990**, *187*, 357.
[35] R. M. A. Azzam, N. M. Bashara, *Ellipsometry and Polarized Light*; North Holland Physics Publishing, Amsterdam, **1979**, p. 354.
[36] J. Schellman, H. P. Jensen, *Chem. Rev.* **1987**, *87*, 1359.
[37] M. J. Tunis-Schneider, M. Maestre, *J. Mol. Biol.* **1970**, *52*, 521.
[38] Recently, Cook and co-workers described the formation of LB films from a phthalocyanine that is mesogenic at elevated temperatures: M. J. Cook, J. McMurdo, D. A. Miles, R. H. Poynter, J. M. Simmons, S. D. Haslam, R. M. Richardson, K. Welford, *J. Mater. Chem.* **1994**, *4*, 1205.
[39] a) M. VandeAuweraer, C. Catry, L. Feng Chi, O. Karthaus, W. Knoll, H. Ringsdorf, M. Sawodny, C. Urban, *Thin Solid Films* **1992**, *210/211*, 39; b) B. Rapp, M. Eberhardt, H. Gruler, *Makromol. Chem. Macromol. Symp.* **1991**, *46*, 439; c) P. A. Albouy, *J. Phys. Chem.* **1994**, *98*, 8543; d) F. Takeda, M. Matsumoto, T. Takenaka, Y. Fujiyoshi, N. Uyeda, *J. Coll. Interf. Sci.* **1983**, *91*, 267; e) M. N. Teerenstra, E. J. Vorenkamp, A. J. Schouten, R. J. M. Nolte, C. A. van Walree, J. F. van der Pol, J. W. Zwikker, *Thin Solid Films* **1992**, *210/211*, 496.

0570-0833/95/0303-0182 $ 30.00+.25/0